Evaluation of delayed-image bone scintigraphy to assess bone formation after distraction osteogenesis in dogs

Lars F. Theyse, VMD; Herman A. Hazewinkel, VMD, PhD; Maarten Terlou, PhD; Yvonne W. Pollak; George Voorhout, VMD, PhD

Objective—To quantitatively assess distraction-induced bone formation in a crural lengthening model in dogs by use of delayed-image bone scintigraphy.

Animals—12 mature Labrador Retrievers.

Procedures—Dogs were randomly allocated to 1 of 3 groups. A circular external skeletal fixation system was mounted on the right crus of each dog. Osteotomy of the distal portion of the tibia and fibula was performed in groups 1 and 2 and was followed by a lengthening procedure of 10 mm in the first group only. The third group served as sham-operated controls. Delayed-image bone scintigraphy with technetium-99m hydroxy methylene diphosphonate was performed 2, 4, and 6 weeks after surgery. Delayed-image–to–region-of-interest, delayed-image–to–crural, and delayed-image–to–femoral scintigraphic activity ratios were calculated. New bone formation was quantified by use of densitometric image analysis, and values for the scintigraphic ratios were compared.

Results—In the distraction and osteotomy groups, values of delayed-image–to–region-of-interest and delayed-image-to-crural ratios increased significantly. Although densitometric image analysis revealed increased bone formation after distraction, the region-of-interest ratios and crural ratios were similar in both groups. All dogs had increased delayed-image–to–femoral ratios.

Conclusions and Clinical Relevance—Delayed-image bone scintigraphy ratios were not effective at differentiating between the amounts of distraction-induced bone and osteotomy-induced bone. Metabolic bone activity in the adjacent femur was increased as a consequence of circular external skeletal fixator placement. Delayed-image bone scintigraphy was not adequately sensitive to quantitatively monitor bone formation but may be useful as an early predictor of bone healing. (*Am J Vet Res* 2006;67:xxx–xxx)

Distraction osteogenesis has been used in the management of various skeletal conditions, including bone length deficits, bone deformities, bone loss after traumatic injury or radical resection, and craniofacial reconstruction.[1,2] The principle of distraction osteogenesis describes formation of new bone under conditions of controlled mechanical distraction of an osteotomy site. Distraction osteogenesis is characterized by intramembranous bone formation.[3,4] In contrast, routine healing at an osteotomy site is initiated with callus formation and proceeds via endochondral bone formation. The extent of distraction osteogenesis is determined by many factors, including the site of the osteotomy, latency period, distraction rate, soft tissue condition, local blood supply, and age of the animal. Blood flow to the area of affected bone is also associated with the rate of osteogenesis.[5] Although histologic, ultrastructural, and radiologic methods to characterize distraction osteogenesis has been described,[6-8] those methods are either invasive or only applicable in later phases of the mineralization process. Delayed-image bone scintigraphy is a noninvasive quantitative method for evaluating changes in bone metabolic activity.[9,10] In contrast to radiography, which reveals the amount of mineralization, delayed-image bone scintigraphy evaluates uptake of technetium-99m tracer by immature bone and thus precedes actual accretion of bone.[11,12] In distraction osteogenesis, delayed-image bone scintigraphy has been used successfully to predict the progression of bone formation in the early stages of the lengthening process and to assess the optimal time of bone consolidation in the later stages of bone maturation.[9,10] We hypothesized that delayed-image bone scintigraphy would be useful in the quantitative assessment of bone regeneration after a distraction osteogenesis procedure. Because distraction osteogenesis is known to increase local and regional blood flow, we also speculated that the lengthening procedure would increase the rate of bone metabolism in the adjacent long bone.[5]

Received September 23, 2005.
Accepted December 1, 2005.

From the Department of Clinical Sciences of Companion Animals (Theyse, Hazewinkel) and the Division of Diagnostic Imaging (Pollak, Voorhout), Faculty of Veterinary Medicine, and the Department of Image Processing and Design, Faculty of Biology (Terlou), Utrecht University, Utrecht, The Netherlands.
Address correspondence to Dr. Theyse.

Abbreviations

CESF	Circular external skeletal fixation
^{99m}Tc-HDP	Technetium-99m hydroxy methylene diphosphonate

Materials and Methods

Animals—Procedures were approved by the Utrecht University Ethical Committee for Animal Care and Use, and all experimentation was conducted in conformity with ethical and humane principles of research. Twelve mature Labrador Retrievers with a mean age of 19 months (range, 12 to 31 months) and mean body weight of 27 kg (range, 21 to 32 kg) were allocated to 1 of 3 groups (n = 4 each). Dogs were individually housed and fed a standard commercial dog food twice a day and had ad libitum access to water.

Surgery and distraction procedures—The lengthening procedure was performed by application of a CESF system.[a] All frames were identical and consisted of 2 proximal and 2 distal full rings with a 100-mm diameter, connected by 3 treaded rods with a 1-mm pitch. Frames were assembled prior to surgery and steam sterilized. Dogs received medetomidine[b] as a preanesthetic sedative, and anesthesia was induced with propofol[c] administered IV. After intubation, inhalation anesthesia with nitrous oxide, oxygen, and isoflurane commenced. Amoxicillin with clavulanic acid[d] was administered (20 mg/kg, IV) prior to surgery. The skin of the right hind limb was aseptically prepared in a standard fashion. A CESF was attached to the right tibia by use of two 1.5-mm diameter transosseous wires on both the proximal and distal rings and one 1.5-mm diameter transosseous wire on both central rings. An equivalent of 60 kg of tension was applied to the wires with a dynamometric wire tensioner.[e]

A craniomedial surgical approach to the tibia and fibula was used to facilitate circumferential elevation of the soft tissues and periosteum. In dogs in the distraction and osteotomy groups, osteotomy of the tibia and fibula was performed in the diaphysis, at the level of two thirds of the tibial length from its proximal aspect, by use of an oscillating saw. Ample volumes of fluids were used for lavage during the osteotomy procedure for thermal protection of the periosteum and osteotomized bone.

Dogs in the control group were sham-operated. In all dogs, the periosteum was closed with absorbable suture material and closure of the subcutis and skin proceeded routinely. Dogs wore a protective full-limb bandage for 3 days after surgery and received buprenorphine[f] (10 µg/kg, SC, q 6 h) as an analgesic for 3 days after surgery. Full loading of the limbs was permitted immediately after surgery. After 4 days, dogs in the distraction group were subjected to lengthening via adjustment of the CESF at a rate of 0.5 mm twice daily for 10 consecutive days. The site of bone regeneration was allowed to mature for an additional 4 weeks. Dogs were euthanatized with a barbiturate overdose 6 weeks after the initial surgery.

Delayed-image bone scintigraphy—Delayed-image bone scintigraphy was performed 2, 4, and 6 weeks after surgery. Each dog received 550 MBq of ^{99m}Tc-HDP, IV, 3 hours before data collection. Scintigraphic imaging was performed with a gamma camera system[g] equipped with a high-resolution parallel-hole collimator. The gamma camera was connected to a dedicated open workstation computer. Immediately prior to scintigraphic imaging, dogs were premedicated with medetomidine and anesthesia was induced and maintained by a continuous rate infusion of propofol delivered via an infusion pump. Dogs were positioned in dorsal recumbency with both crura placed parallel to the tabletop. The camera was positioned over both hind legs with the collimator centered over the distraction zone, osteotomy zone, or corresponding zone in the control group, perpendicular to the long axis of the right and left crura. Counts were collected during a 5-minute period by use of a 256 X 256 matrix with a pixel size of 1.68 mm. Simultaneously, 1 mL of a dilution of the injection dose (dilution, 1:1,000) was counted and used as a standard. Bone metabolic activity was determined (by focusing the camera on the distraction, osteotomy, and control zones) for the region of interest, the entire crus, and the distal one third of the femur. The regions of interest were selected to include the area of all mineralized callus that was radiographically visible adjacent to the osteotomy zone 6 weeks after surgery. The region of interest was centered over the osteotomy zone with an equal distribution over the proximal and distal segments of the bone. The dimensions of the region of interest were 20 X 10 pixels (5.64 cm^2). An identical region of interest was used for the opposite limb. The same regions of interest were used in the sham-operated dogs. In the distraction group, the region of interest on the right (experimental) limb was enlarged in a proximodistal direction to 20 X 16 pixels (9.03 cm^2) to include the same amount of original crural bone as was included in dogs in the osteotomy and control groups as well as the area of distraction-induced bone regeneration in the lengthening zone. The region of interest for the left limb remained the same as that in dogs in the other groups. The precise locations of the regions of interest were chosen with reference to the radiographs of each dog so that the same anatomic area evaluated in the densitometric image analysis was accurately reflected.

Activity in the entire tibia and fibula (ie, crural activity) on the right and left limbs was measured. The distal one third of the femur (ie, femoral activity) was delineated on the scans, and that activity was measured (**Figure 1**). Activity in the right and left limbs was expressed as a percentage of total dose activity. The dose percentage of activity in the right limb was divided by that in the left limb to yield a ratio that expressed the difference in bone metabolic activity between the 2 limbs. Thus, the delayed-image–to–region-of-interest ratio, delayed-image–to–crural ratio, and delayed-image–to–femoral ratio were determined.

Densitometric image analysis—Densitometric image analysis of radiographs was used to measure new bone formation.[13] Immediately after surgery and once weekly for 6 weeks thereafter, radiographs of the right crus and CESF were obtained in the caudocranial and lateromedial planes. The radiographic views included a ruler and an aluminum step-wedge consisting of ten 2-mm thick aluminum slabs mounted in an overlapping manner. Bone formation was quantified by use of a densitometric image analysis system. Radiographs were recorded with a high-resolution charge coupled device camera[h] and digitalized for image analysis (frame size, 752 X 574 pixels; 256 gray levels) with a personal computer–based system equipped with imaging software.[i] A program was developed to quantify the amount of mineralized callus observed. Each radiograph was calibrated geometrically and densitometrically by use of the image of the ruler and aluminum step wedge. The densitometric calibration was performed by measuring the mean optical densi-

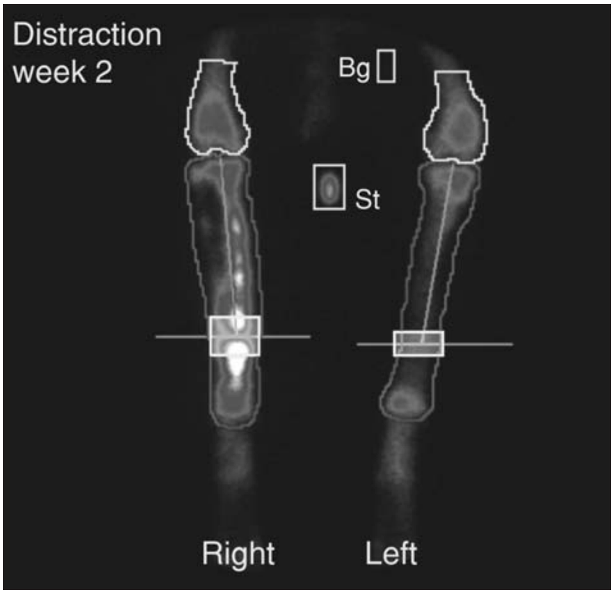

Figure 1—Delayed-image bone scintigraphic images of the right and left crura and distal portion of the femurs in a dog that underwent an osteotomy procedure and postoperative distraction osteogenesis. The region of interest (highlighted), entire crus, and distal portion of the femur are outlined. Notice the area of high uptake of ^{99m}Tc-HDP tracer adjacent to and in the distraction zone in the distal portion of the experimental (right) tibia. St = Standard. Bg = Background.

ty of a square area of 50 X 50 pixels in 6 steps of the aluminum model (ie, 0, 2, 4, 6, 8, and 10 mm). Measurements were obtained from a median-filtered image to reduce the influence of photographic grain in the film. The optical density values were fit polygonally with the aluminum values to yield a transformation table, which enabled expression of the amount of newly formed bone in units of equivalents of cubic millimeters of aluminum. The region of interest was centered over the distraction or osteotomy zone as was performed in the delayed-image bone scintigraphy procedure and included all new bone formation. The regions of interest were delineated on the digitalized caudocranial and lateromedial images, and densitometric analyses (including the bone area and bone amount) were performed. For each dog, mean bone area and bone amount in the caudocranial and lateromedial images were determined and used for statistical analysis.

Statistical analysis—Delayed-image ratios were evaluated via ANOVA for repeated measures and a least significant difference post hoc test. Densitometric data, including values for bone area and bone amount, were compared by use of a Student *t* test. Correlations between delayed-image ratios and densitometric bone area and bone amount were examined by use of the Pearson correlation test. Power was set at 0.80, and values of $P < 0.05$ were considered significant. Analyses were performed by use of commercially available statistical software.[j]

Results

Scintigraphy—Bone metabolic activity was significantly higher on the instrumented right side in all dogs in the distraction, osteotomy, and control groups. The higher uptake of ^{99m}Tc-HDP resulted in increased delayed-image–to–region-of-interest ratios, delayed-image–to–crural ratios, and delayed-image–to–femoral ratios at all time points. In the distraction group, the mean region-of-interest ratio initially had the largest increase but values were not significantly different from those in the osteotomy group (**Figure 2**). Dogs in both the distraction and osteotomy groups had significantly higher mean delayed-image–to–region-of-interest ratio than controls at all time points. Although delayed-image–to–crural ratios were highest in the distraction group, the differences between those ratios and ratios in the osteotomy group were not significantly different (**Figure 3**). The distraction and osteotomy groups had significantly higher delayed–image–to–crural ratios than controls at all time points. Although delayed-image–to–femoral ratios indicated a higher uptake of ^{99m}Tc-HDP in the femurs of instrumented limbs, compared with the contralateral limbs, no differences were observed among groups (**Figure 4**). Delayed-image ratios of the region of interest, crus, and femur tended to increase during the study period.

Densitometric image analysis—The distraction procedures were uneventful in all dogs, and no complications were encountered. In dogs in the distraction and osteotomy groups, periosteal new bone adjacent to the osteotomy site was observed radiographically as early as 1 week after surgery. The amount and density of periosteal bone increased over time. In the distraction zone, new bone formation was observed 3 weeks after surgery and periosteal bone had merged with

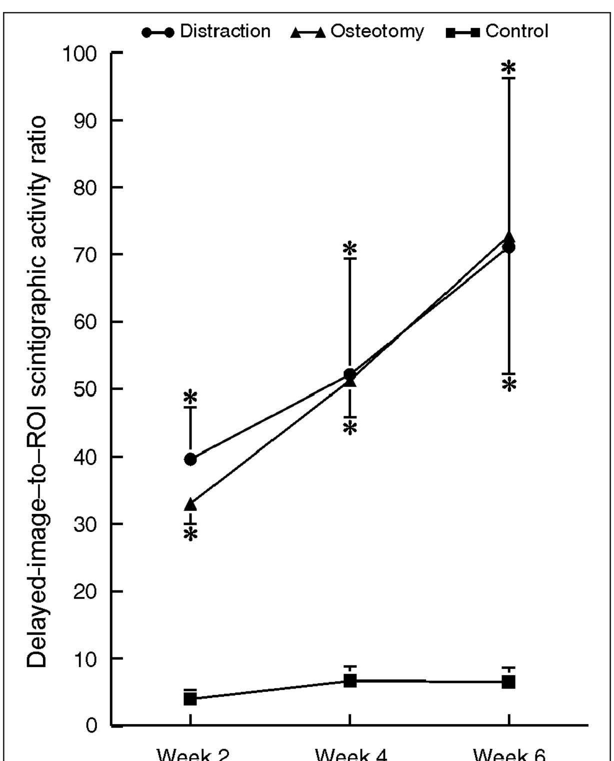

Figure 2—Changes in delayed-image–to–region-of-interest (ROI) scintigraphic activity ratios after surgery in 12 dogs that underwent osteotomy alone (n = 4), osteotomy and distraction osteogenesis (4), or a sham procedure (4). Delayed-image– to– ROI ratios were calculated as activity in the ROI as a percentage of total dose activity. Data are presented as mean ± SEM. *Significantly ($P < 0.05$) higher than value for controls.

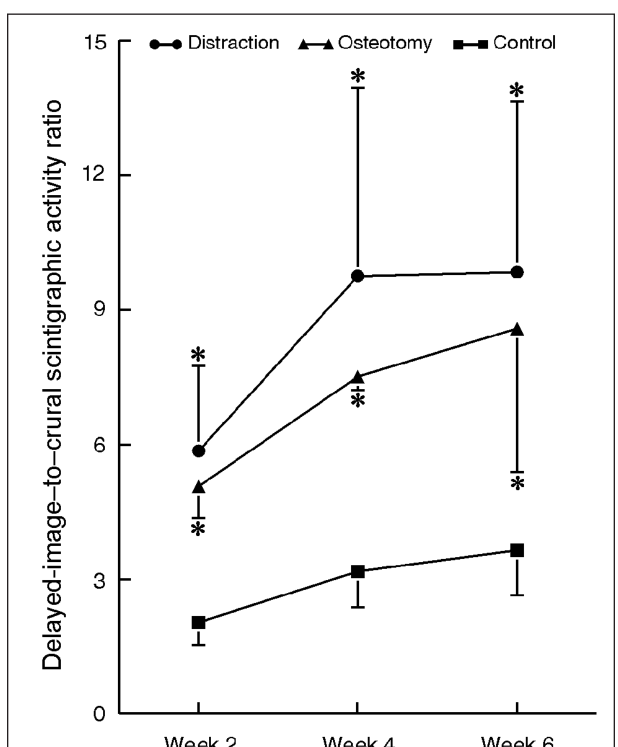

Figure 3—Changes in delayed-image–to–crural scintigraphic activity ratios in the same dogs as in Figure 2. Data are presented as mean ± SEM. *Significantly ($P < 0.05$) higher than value for controls.

bone in the distraction zone at 4 weeks. In the control dogs, no periosteal bone formation was detected at the site of periosteal elevation. Mineralization in dogs in the distraction and osteotomy groups had progressed to an extent that densitometric evaluation was possible beginning in week 5. In the distraction group, measurements of bone area and bone amount were significantly larger 5 and 6 weeks after surgery, compared with measurements in the osteotomy group. In dogs in the distraction group, bone area and bone amount increased during that period (**Table 1**).

The mean delayed-image–to–region-of-interest ratio in the distraction group was positively correlated with densitometric bone area, but not with the densitometric bone amount, at 6 weeks (R = 0.95; $P = 0.02$ and R = 0.84; $P = 0.08$, respectively). In the osteotomy group, no significant correlations were detected between the delayed-image–to–region of interest ratio versus bone area or bone amount (R = 0.61, $P = 0.20$ and R = 0.65; $P = 0.18$, respectively).

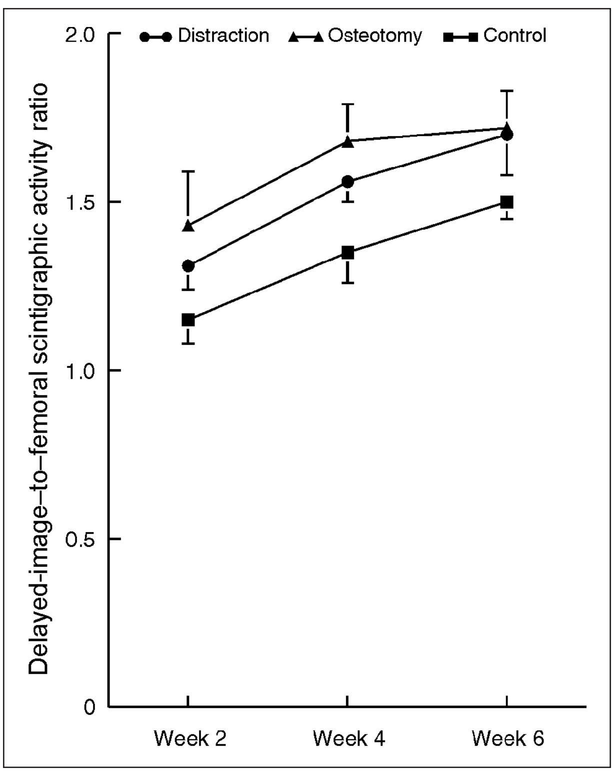

Figure 4—Changes in delayed-image–to–femoral scintigraphic activity ratios in the same dogs as in Figures 2 and 3. Data are presented as mean ± SEM. Notice that there were no significant differences in values among the groups.

Discussion

We hypothesized that delayed-image bone scintigraphy would be useful in quantitatively assessing bone regeneration after a distraction osteogenesis procedure. We also speculated that a lengthening procedure would increase bone metabolic activity in the adjacent long bone. Delayed-image bone scintigraphy ratios were not effective in quantitatively differentiating between distraction-induced bone formation and osteotomy-induced bone formation. Metabolic bone activity in the adjacent femur was increased as a consequence of placement of the CESF device.

Dogs in this study had no prior bone disease or injury and all healed without complication, but results in a clinical setting could be different. Radiographic data revealed the lengthening procedure to be successful via analogy with previous models[4,14] of distraction osteogenesis in dogs and other species. In the present study, an oscillating saw and high-volume lavage were used during the osteotomy, a technique that has been effective in experimental and clinical settings.[6,15-17] Densitometric image analysis revealed a greater amount of bone formation in association with the distraction procedure, compared with bone formation after osteotomy alone.

Three-phase bone scintigraphy is a noninvasive method for semiquantitative assessment of blood flow, blood distribution, and bone metabolic activity.[11] Angiographic imaging during 3-phase scintigraphy reflects local blood perfusion. Hyperemia of bone and soft tissues is revealed on the blood-pool image. Accumulation of ^{99m}Tc-HDP in the delayed image was presumed to reflect osteoblast activity and new bone formation. Many studies[5,10,18-21] have revealed that blood flow increases during the processes of bone healing and distraction osteogenesis. Although blood supply is considered to be closely related to rate of osteogenesis, blood flow, as indicated by the perfusion index, appears to be of questionable value as a predictor of new bone formation.[9,10,22] In contrast to the information yielded in the first 2 phases of bone scintigraphy, the value of delayed-image bone scintigraphy in predicting the outcome of bone consolidation after a distraction procedure in humans has been reported.[10] Recent studies[23-26] have revealed the role of angiogenic factors, including vascular endothelial growth factor and basic fibroblast growth factor, in distraction-induced bone regeneration. Expression of those factors is maximal during active bone lengthening and decreased during the consolidation phase.

In the present study, we used delayed-image bone scintigraphy to determine the activity of bone metabo-

Table 1—Summary of densitometric image data for new bone formation in dogs that underwent an osteotomy procedure alone (n = 4 dogs) or osteotomy and distraction osteogenesis (4). Measurements were taken 5 and 6 weeks after surgery.

	Bone area (mm^2)		Bone amount (mm^3 Al $\times 10^3$)	
Group	**Week 5**	**Week 6**	**Week 5**	**Week 6**
Distraction	277.6 ± 39.7*	366.6 ± 52.8*, †	278.0 ± 50.7*	365.6 ± 67.0*, †
Osteotomy	120.6 ± 18.8	149.0 ± 26.7	132.9 ± 24.5	166.5 ± 32.7†

Data are given as mean ± SEM.

*Significant ($P < 0.05$) differences between the 2 groups at the corresponding time. †Significant ($P < 0.05$) increase in time within the group.

lism and new bone formation during a lengthening procedure. Initially, the delayed-image–to–region of interest ratio was increased most notably in dogs in the distraction group. This point in time coincided with the end of active lengthening, which is characterized by the highest expression of angiogenic and osteotropic growth factors (eg, bone morphogenetic proteins, insulin-like growth factor I, and transforming growth factor β) and thus the highest rate of bone formation.[26-31] Because densitometric image analysis revealed the mean area of new bone formation in the distraction group to be more than twice the size of that in the osteotomy group 6 weeks after surgery, we expected that the delayed-image–to–region-of-interest ratio would reveal this difference. Whether the lack of increase in the region-of-interest ratio can be attributed to a different rate of uptake of ^{99m}Tc-HDP during intramembranous bone formation is uncertain.[3,4] Another explanation is that there could have been altered distribution of tracer as a result of increased blood flow in the lengthened crus. Nevertheless, observation of increasing delayed-image–to–region-of-interest ratios from week 2 onwards in both the distraction and osteotomy groups was consistent with the radiographic evidence of advancing bone formation.[9]

The strong correlation between the delayed-image–to–region-of-interest ratio and densitometric bone area, but not bone amount, in the distraction group at 6 weeks was consistent with the assumption that counts obtained in delayed-image bone scintigraphy are not a measure of mineralization. Although delayed-image–to–region-of-interest ratios were similar in the distraction and osteotomy groups, delayed-image-to-crural ratios tended to be higher after distraction throughout the study period. Upregulation of bone metabolism outside the lengthening zone, mediated via production of osteotropic and angiogenic growth factors during the distraction procedure, may play a role in this finding.[26-32] Potentially significant differences between the regions of interest may have been obscured by the sample size in the present study, but differences would be less relevant, compared with results of densitometric image analysis.

In the control group, the effect of the CESF system on bone response in the right limbs suggested that the metabolic response of bone to a minimally invasive external fixator can be substantial. Whether enhanced bone metabolic activity was the result of production of angiogenic and osteotropic growth factors as a reaction to the transosseous wires is unclear. Although the local response, characterized by the delayed-image–to–region-of-interest ratios and delayed-image-to-crural ratios, differed significantly in both the distraction and osteotomy groups, compared with controls, the distant effect on the femur was of similar magnitude in all 3 groups. In actively growing dogs, the increased bone metabolism in the adjacent long bone during distraction osteogenesis or fracture healing could be responsible for the phenomenon of longitudinal bone growth stimulation.[33-35]

In summary, delayed-image bone scintigraphy ratios were not effective in quantitatively differentiating between the amount of distraction-induced versus osteotomy-induced bone formation. Delayed-image–to–region-of-interest and delayed-image-to-crural ratios revealed bone formation in the areas of distraction-induced activity and bone callus at the osteotomy site. In the clinical setting, delayed-image bone scintigraphy ratios may be valuable as early predictors of bone healing. Nevertheless, quantification of newly formed bone in individual patients does not appear to be feasible. Instrumentation with a CESF system appears to stimulate bone metabolism not only in the instrumented bone but also in adjacent long bones.

a. Imex Veterinary Inc, Longview, Tex.
b. Domitor, Pfizer Animal Health BV, Capelle a/d IJssel, The Netherlands.
c. Rapinovet, Schering-Plough Animal Health NV, Bruxelles, Belgium.
d. Augmentin, SmithKline Beecham Farma BV, Rijswijk, The Netherlands.
e. Hofmann SaS, Monza, Italy.
f. Temgesic, Schering-Plough, Weesp, The Netherlands.
g. Siemens Medical Systems, Den Haag, The Netherlands.
h. Sony b/w CCD camera type XC-77CE, Sony Corp, Tokyo, Japan.
i. KS400, version 3.0 software, Carl Zeiss Vision, Oberkochen, Germany.
j. SPSS 10.1 statistical package, SPSS Inc, Chicago, Ill.

References

1. Maffulli N, Lombari C, Matarazzo L, et al. A review of 240 patients undergoing distraction osteogenesis for congenital post-traumatic or postinfective lower limb length discrepancy. *J Am Coll Surg* 1996;182:394–402.
2. Stanitski DF, Shahcheraghi H, Nicker DA, et al. Results of tibial lengthening with the Ilizarov technique. *J Pediatr Orthop* 1996;16:168–172.
3. Aronson J. Experimental and clinical experience with distraction osteogenesis. *Cleft Palate Craniofac J* 1994;31:473–481.
4. Aronson J, Good B, Stewart C, et al. Preliminary studies of mineralization during distraction osteogenesis. *Clin Orthop Relat Res* 1990;250:43–49.
5. Aronson J. Temporal and spatial increases in blood flow during distraction osteogenesis. *Clin Orthop Relat Res* 1994;301:124–131.
6. Delloye C, Delefortrie G, Coutelier L, et al. Bone regenerate formation in cortical bone during distraction lengthening. An experimental study. *Clin Orthop Relat Res* 1990;250:34–42.
7. Orbay JL, Frankel VH, Finkle JE, et al. Canine leg lengthening by the Ilizarov technique. A biomechanical, radiologic, and morphologic study. *Clin Orthop Relat Res* 1992;265–273.
8. Richards M, Goulet JA, Weiss JA, et al. Bone regeneration and fracture healing. Experience with distraction osteogenesis model. *Clin Orthop Relat Res* 1998;suppl 355:S191–S204.
9. Felemovicius J, Ortiz-Monasterio F, Gomez-Radillo LS, et al. Determining the optimal time for consolidation after distraction osteogenesis. *J Craniofac Surg* 2000;11:430–436.
10. Kawano M, Taki J, Tsuchiya H, et al. Predicting the outcome of distraction osteogenesis by 3-phase bone scintigraphy. *J Nucl Med* 2003;44:369–374.
11. Nutton RW, Fitzgerald RH Jr, Kelly PJ. Early dynamic bone-imaging as an indicator of osseous blood flow and factors affecting the uptake of 99mTc hydroxymethylene diphosphonate in healing bone. *J Bone Joint Surg Am* 1985;67:763–770.
12. van Roermund PM, Hoekstra A, Ter Haar-Romeny BM, et al. Bone healing during lower limb lengthening by distraction epiphysiolysis. *J Nucl Med* 1988;29:1259–1263.
13. Fink B, Fox F, Singer J, et al. Monitoring of bone formation during distraction osteogenesis via osteocalcin: a time sequence study in dogs. *J Orthop Sci* 2002;7:557–561.
14. Frierson M, Ibrahim K, Boles M, et al. Distraction osteogenesis. A comparison of corticotomy techniques. *Clin Orthop Relat Res* 1994;301:19–24.
15. Marcellin-Little DJ. Treating bone deformities with circular

external skeletal fixation. *Compend Contin Educ Pract Vet* 1999; 21:481–491.

16. Latte Y. 75 applications of the Ilizarov method (part 2). *Eur J Comp Anim Pract* 1998;8:64–81.

17. Marcellin-Little DJ, Ferretti A, Roe SC, et al. Hinged Ilizarov external fixation for correction of antebrachial deformities. *Vet Surg* 1998;27:231–245.

18. Aalto K, Slatis P. Blood flow in rabbit osteotomies studied with radioactive microspheres. *Acta Orthop Scand* 1984; 55:637–639.

19. Minematsu K, Tsuchiya H, Taki J, et al. Blood flow measurement during distraction osteogenesis. *Clin Orthop Relat Res* 1998;347:229–235.

20. Mueller M, Schilling T, Minne HW, et al. A systemic acceleratory phenomenon (SAP) accompanies the regional acceleratory phenomenon (RAP) during healing of a bone defect in the rat. *J Bone Miner Res* 1991;6:401–410.

21. Smith SR, Bronk JT, Kelly PJ. Effect of fracture fixation on cortical bone blood flow. *J Orthop Res* 1990;8:471–478.

22. Averill SM, Johnson AL, Chambers M, et al. Qualitative and quantitative scintigraphic imaging to predict fracture healing. *Vet Comp Orthop Traumatol* 1999;12:142–150.

23. Carvalho RS, Einhorn TA, Lehmann W, et al. The role of angiogenesis in a murine tibial model of distraction osteogenesis. *Bone* 2004;34:849–861.

24. Fang TD, Salim A, Xia W, et al. Angiogenesis is required for successful bone induction during distraction osteogenesis. *J Bone Miner Res* 2005;20:1114–1124.

25. Hu J, Zou S, Li J, et al. Temporospatial expression of vascular endothelial growth factor and basic fibroblast growth factor during mandibular distraction osteogenesis. *J Craniomaxillofac Surg* 2003;31:238–243.

26. Pacicca DM, Patel N, Lee C, et al. Expression of angiogenic factors during distraction osteogenesis. *Bone* 2003;33:889–898.

27. Eingartner C, Coerper S, Fritz J, et al. Growth factors in distraction osteogenesis. Immuno-histological pattern of TGF-beta1 and IGF-I in human callus induced by distraction osteogenesis. *Int Orthop* 1999;23:253–259.

28. Farhadieh RD, Dickinson R, Yu Y, et al. The role of transforming growth factor-beta, insulin-like growth factor I, and basic fibroblast growth factor in distraction osteogenesis of the mandible. *J Craniofac Surg* 1999;10:80–86.

29. Farhadieh RD, Gianoutsos MP, Yu Y, et al. The role of bone morphogenetic proteins BMP-2 and BMP-4 and their related postreceptor signaling system (Smads) in distraction osteogenesis of the mandible. *J Craniofac Surg* 2004;15:714–718.

30. Rauch F, Lauzier D, Croteau S, et al. Temporal and spatial expression of bone morphogenetic protein-2, -4, and -7 during distraction osteogenesis in rabbits. *Bone* 2000;27:453–459.

31. Tavakoli K, Yu Y, Shahidi S, et al. Expression of growth factors in the mandibular distraction zone: a sheep study. *Br J Plast Surg* 1999;52:434–439.

32. Hansen-Algenstaedt N, Algenstaedt P, Bottcher A, et al. Bilaterally increased VEGF-levels in muscles during experimental unilateral callus distraction. *J Orthop Res* 2003;21:805–812.

33. Sabharwal S, Paley D, Bhave A, et al. Growth patterns after lengthening of congenitally short lower limbs in young children. *J Pediatr Orthop* 2000;20:137–145.

34. Holbein O, Neidlinger-Wilke C, Suger G, et al. Ilizarov callus distraction produces systemic bone cell mitogens. *J Orthop Res* 1995;13:629–638.

35. Kaspar D, Neidlinger-Wilke C, Holbein O, et al. Mitogens are increased in the systemic circulation during bone callus healing. *J Orthop Res* 2003;21:320–325.